

Multipath Mitigation on In Situ Communication Links

L. Tadjpour¹ and D. Bell¹

On both ends of an in situ ultra-high frequency (UHF) link, multipath signal reflections—characterized by signal reflection, diffraction, and blockage—can cause a significant drop in link performance. The purpose of this article is to study the extent and effects of multipath signal reflections, explore possible strategies, and provide recommendations for mitigating multipath for communications over a relay link. The performance of telecommunications over a relay link with different antenna options on both ends was studied. Results of our analysis and simulations indicate that keeping the antenna pattern symmetric is important. It was shown that data-return volume for a Smart Lander communicating with Odyssey increases over 2.6 dB if the monopole antenna is placed on the equipment deck rather than on the solar arrays. In similar scenarios, data-return volume improves some 0.4 dB if a cross-dipole antenna is used on the rover instead of an equipment-deck-mounted monopole antenna on the rover. The reason is that horizontally/circularly polarized antennas reduce the coupling to the vertical scatterers on the rover and hence maintain a more symmetric pattern on different locations of the rover. In summary, the spacecraft layout and antenna placement should strive to minimize impacts that would create antenna-pattern asymmetry. The effects of Mars' environment on the relay uplink performance also was studied. Received signal-power variations as a function of satellite elevation angle and azimuth angle were calculated for the Mars Exploration Rover (MER), located in Martian open, flat terrain and Martian hilly terrain, communicating uplink to the spacecraft. It was shown that despite the monopole and cross-dipole discrimination against multipath, signal variation can reach -13 dB at elevation angles between 5 and 15 deg. Cross-dipole antennas impose more discrimination at low elevation angles than do monopole antennas. It was observed that using a cross-dipole antenna instead of a monopole antenna on MER decreases signal variation, especially at larger elevation angles.

I. Introduction

Multipath signal reflections—characterized by signal reflection, diffraction, and blockage—can cause significant signal variations in the received signal power of the spacecraft and the rover. Multipath creates “holes” in the antenna beam pattern that cause the signal to drop out. This makes telecommunications

¹ Communications Systems and Research Section.

The research described in this publication was carried out by the Jet Propulsion Laboratory, California Institute of Technology, under a contract with the National Aeronautics and Space Administration.

operations planning more difficult. In addition, a rover moves in relation to its environment, changes its orientation, and may even deploy and retract various subsystems. The result is variable multipath effects that can move the task of telecommunications operations planning from the realm of difficult to impossible.

The situation on the spacecraft end of the link is not much better. Variations in spacecraft attitude and in the positions and orientations of RF reflective subsystems, such as the high-gain antenna (HGA) and solar arrays, can also modify the ultra-high frequency (UHF) antenna gain pattern. The link availability and uncertainty are particularly problematic for support of special events like entry, descent, and landing (EDL), for which there is only one opportunity to capture essential data. Matters are further complicated by mechanical designers who place antennas in poor locations and orientations, either out of ignorance or in anticipation of mass and volume saving. Moreover, distortion of the antenna patterns also reduces RF isolation between the UHF telecommunications subsystem and science packages.

Finally, surrounding objects reflect, scatter, or diffract transmitting signals, which leads to unwanted signal variations.

This article investigates the effects of multipath on the in situ links and suggests practical measures for mitigating multipath. The article is organized in the following manner: Section II investigates the effect of multipath on the antenna gain pattern on the rover. Trade-offs involved in using different antennas on the rover are investigated. Section III investigates the impact of low-gain UHF antenna placement on the orbiter. Section IV explores the extent and effects of multipath from the Martian environment.^{2,3}

II. Effects of Multipath on the Antenna Gain Pattern Mounted on the Rover

Extensive studies have been carried out to examine the UHF antenna specifications for the Mars Exploration Rover (MER).^{4,5} Figure 1 shows a monopole antenna on the MER new mockup. The panoramic camera is located on the top of the rover equipment deck (RED), covered by blue solar cells, and the high-gain antenna (HGA) and low-gain antenna (LGA) are mounted on the bottom. The aluminum sheet (the gray sheet in Fig. 1) was used for solar panels and is to be covered by solar arrays. The UHF $\lambda/4$ monopole with a 0.635-cm diameter is mounted on the solar arrays. The monopole antenna is the most popular antenna and has been used in various applications. It is wide beam, low cost, and can easily be fed. Figure 2 shows the contour plot of the monopole gain pattern mounted on the solar arrays. All points on the elevation rings (three of them are shown in the figure) have constant elevation angles. Note that 0-deg elevation is the zenith because of the way the MER mockup is mounted. In other words, the elevation angle here is equivalent to the off-bore-sight angle. Each plot of a set shows a different “pol angle.” The pol angle is the *azimuth* angle used for that particular cut taken in the measurement. There are 18 cuts per each set of elevation angles or 1 azimuth-angle cut every 10 deg. A nineteenth, the 180-deg cut is taken to verify that the 180-deg cut matches the 0-deg cut flipped left to right. The values of gain pattern in dBi specify the color in each cell of the plot; the color bar is shown on the side of the plot. This is a typical result for many locations of the monopoles on the rover and for many monopole types.

Figure 3 is a one-dimensional plot of monopole antenna gain versus elevation angle for three given azimuth angles. If the antenna pattern were uncorrupted by its surroundings, we would expect a gain

² J. Vacchione, P. Brown, J. Huang, K. Kelly, and M. Thelen, “Antenna Subsystem Peer Review,” JPL internal document, Jet Propulsion Laboratory, Pasadena, California, May 3, 2001.

³ M. Danos and A. Barbieri, “Performance of 2001 Mars Odyssey Relay Link with Monopole and Balun Fed Turnstile Antenna Options for the Mars Exploration Rover (MER),” JPL Interoffice Memorandum 3312-01-0004 (internal document), Jet Propulsion Laboratory, Pasadena, California, June 2001.

⁴ J. Vacchione et al., op cit.

⁵ M. Danos et al., op cit.



Fig. 1. The monopole antenna on the new MER mock-up.

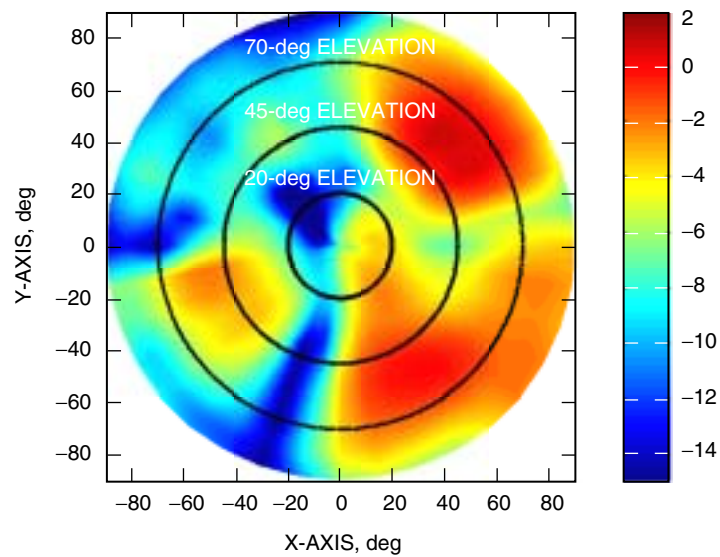


Fig. 2. Contour plot of the monopole antenna on the MER solar array at 415.1 MHz.

pattern symmetrical in azimuth and all three of these curves to fall on top of each other. In other words, the gain of a monopole antenna in infinite space would increase from zero at zenith to a maximum at 90-deg off-bore-sight angles. The fact that there is such variance results from the poor placement of this antenna. Specifically, interactive RF coupling and multipath from nearby metallic structures corrupt the monopole pattern.

Extensive simulations and experimental studies performed by the MER design team yielded the conclusion that a monopole antenna mounted on the rover equipment deck would have a much more symmetrical pattern. The contour plot of the monopole on the RED is shown in Fig. 4.

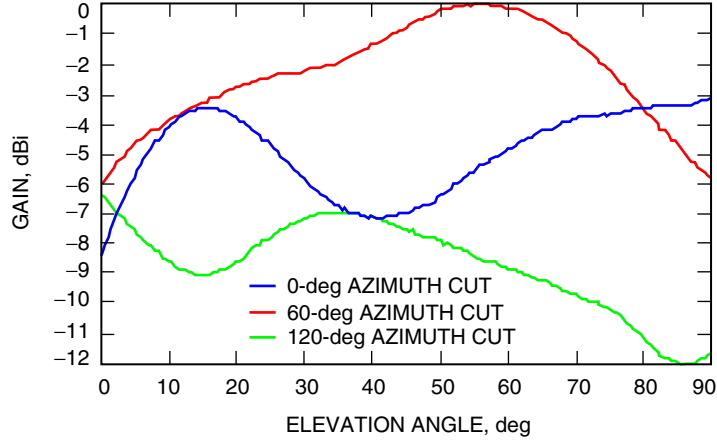


Fig. 3. Monopole antenna gain on the MER solar array versus elevation angle.

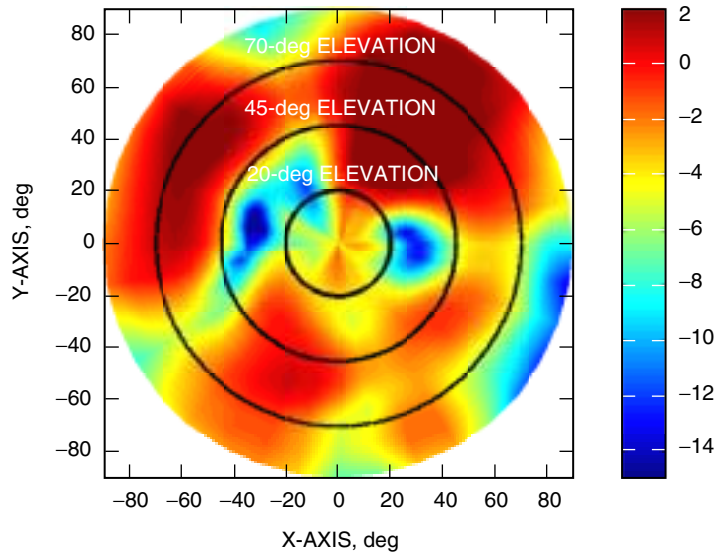


Fig. 4. Contour plot of the monopole antenna on the MER equipment deck at 415.1 MHz.

Any vertically polarized antenna, such as a monopole antenna, causes significant currents on rover components that are tall, slender, and vertical (the LGA, the panoramic camera, and parts of the HGA). These vertical elements will become parasitic antenna elements and corrupt the pattern of the monopole UHF antenna. Moreover, there will be approximately 3 dB lost in linking with a right-hand circularly polarized wave from the orbiter antenna. Deploying a horizontally/circularly polarized antenna would capture some of the 3 dB lost in linking with a right-hand circularly polarized orbiter antenna and reduce the coupling to the vertical elements on the rover. Figure 5 shows a balun-fed, circularly polarized turnstile (cross-dipole) antenna mounted on the MER solar array. The cross-dipole antenna consists of four dipole elements, as shown in Fig. 5. The equal-amplitude signals are fed to the two orthogonal arms with a $\pi/2$ in-phase difference. A cross-dipole antenna requires a balun be excited by coaxial cables, which is an unbalanced feed line. Furthermore, a 3-dB hybrid (power divider) generally is used to feed a cross-dipole antenna in order to be able to feed the same power and a phase difference of $\pi/2$ for each arm. Also, a balun-fed turnstile does not easily fit in the rover in the stowed configuration and requires deployment. A typical gain contour plot of a balun-fed turnstile also is shown in Fig. 6. Much better symmetry in



Fig. 5. The cross-dipole antenna on the MER solar array.

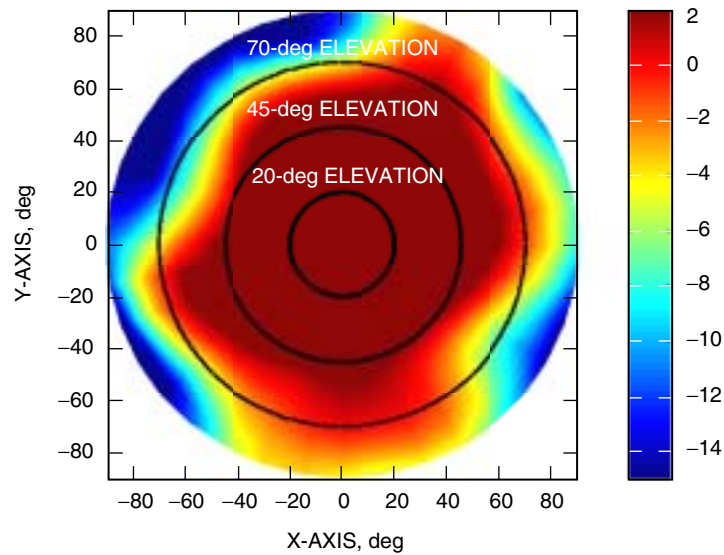


Fig. 6. Contour plot of the cross-dipole antenna mounted on the solar array at 415.1 MHz.

azimuth for this antenna proves that it is a better design than the monopole antenna. Moreover, it has been found that the cross-dipole antenna has robust pattern integrity as a function of location on the rover.

To justify using a better antenna, the data-return benefits of its use must be compared with its additional cost. Figure 7 shows the estimated data-return volume per sol for the Odyssey 2008–Smart Lander uplink. Odyssey uses a quadrafil helix antenna and supports four data rates: 8, 32, 128, and 256 kb/s. It was assumed to have a 1-dB circuit loss. The monopole antenna on the solar array, the monopole antenna on the RED, and the cross-dipole antenna described above were assumed to be mounted on the Smart Lander. The Smart Lander’s location on Mars was assumed to be 160 deg east and 15 deg

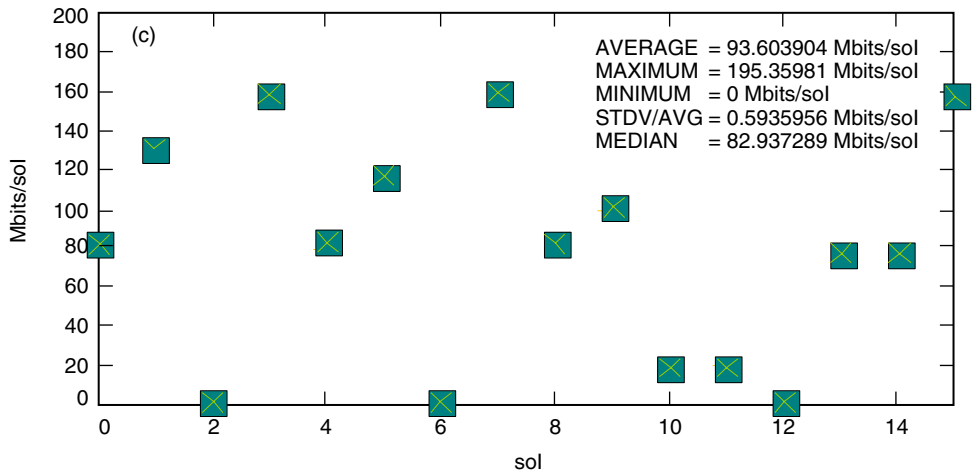
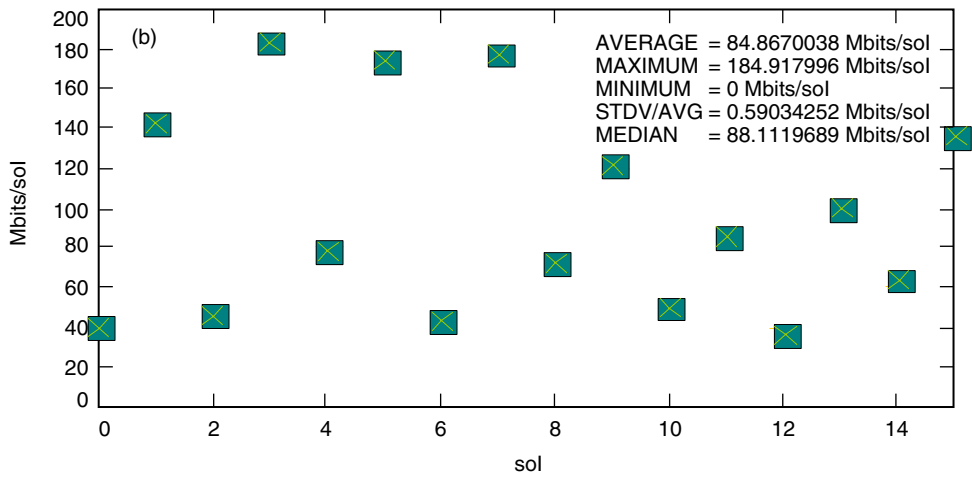
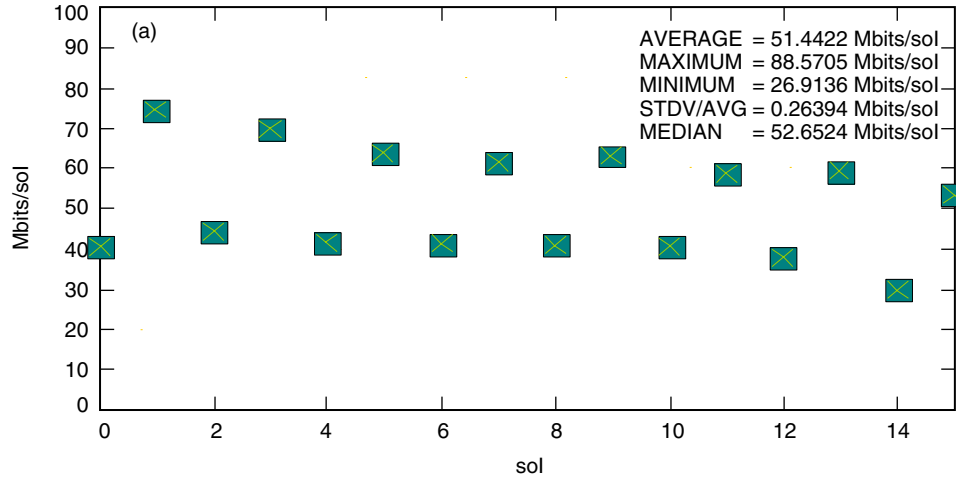


Fig. 7. Odyssey-Smart Lander, data volume versus sol: (a) the solar-array-mounted monopole, 128 kb/s, (b) the equipment-deck-mounted monopole, 256 kb/s, and (c) the cross-dipole antenna, 256 kb/s. (STDV/AVG = standard deviation/average.)

north. It was assumed to have 10 W of transmitted power with a 1-dB uplink circuit loss, and, in the link-budget calculation, a link margin of 3 dB was assumed. Simulation was carried out over 70 sols in order to have a good estimate of the data volume. In each case, several uplink data rates were tried and a single data rate that maximized the average data volume per sol was selected. The minimum required orbiter elevation angle for a successful pass was assumed to be 20 deg. Through Satellite Orbit Analysis Program (SOAP) simulations of geometry, the number of missed passes and the durations of successful passes can be easily obtained. Through link analysis in Excel—and given the threshold value of the orbiter received power that resulted from the link-budget calculation—the contact time (the time in each pass during which the orbiter received power exceeds the threshold) at any data rate was estimated. Data-volume return per pass is the product of the contact time and the corresponding data rate. Data-volume return per sol can be obtained by the product of data rate and the total contact time per sol.

The three curves shown in Fig. 7 have different distributions of data volume over the sol, mainly due to different antenna patterns mounted on the rover. Also, note that the improvement in data-volume return for equipment-deck-mounted monopole and cross-dipole antennas was gained with a data rate of 256 kb/s, which is two times as much as the optimum data rate that the rover with a solar-array-mounted monopole can support. Although with a higher data rate there might be some passes with very low values of data-volume return, the average data volume increases with the deployment of a more symmetric antenna on the rover. Results show that by mounting a monopole antenna on the equipment deck instead of on the solar arrays the average data-volume return of Odyssey–Smart Lander increases 2.17 dB. Deploying a cross-dipole antenna on the rover increases the average data volume 2.6 dB with respect to the solar-array-mounted monopole antenna. However, only a 0.4-dB improvement in data-volume return would be achieved if a cross-dipole antenna were used rather than the equipment-deck-mounted monopole. Thus, it can be concluded that better antenna placement on the rover is more important than what type of antenna is used. This conclusion is strengthened by considering the complexity and mass required to deploy a cross-dipole antenna on the rover.

Figure 8 shows plots of data volume per pass versus maximum elevation angle. Usually, passes with higher maximum elevation angles return higher data volume because the distance between the satellite and the rover decreases and the total contact time during those pass increases. For a perfectly symmetrical antenna pattern, the contact time in each pass is very close to the time during which the rover can see the orbiter. As was said before, a minimum elevation angle of 20 deg is assumed for a successful pass. The blue curves in Fig. 8 are the maximum achievable data-volume return that can be obtained by multiplying the data rate and the fraction of time in each pass when the orbiter elevation angle is above 20 deg. Since in practice this is not the case, the actual data volume per pass does not monotonically increase with elevation angle like the maximum data-volume return curve. However, if an antenna with a more symmetric pattern were placed on the rover, the actual data volume would have values very close to those of the maximum data-volume return. Results show that the cross-dipole antenna case (the yellow curve) follows the blue curve more closely than does the monopole antenna.

III. Effects of Multipath on the Spacecraft Antenna Gain Pattern

In Section II, the results of the simulations of the uplink Odyssey–Smart Lander scenarios were presented. The Odyssey UHF antenna is a low-gain quadrafilary helix antenna. Figure 9 depicts the contour plot of the helix antenna mounted on Odyssey. The plot indicates that the quadrafilary helix mounted on Odyssey maintains its symmetric pattern even in difficult spacecraft environments. Like the cross-dipole antenna, the quadrafilary helix antenna is a circularly polarized antenna. Thus, the vertical RF components on the spacecraft have less adverse effects on its pattern. However, there might be better antenna-placement strategies in order to further reduce the effect of multipath.

Test results indicate that usually the antenna has to be placed away from other RF components of a spacecraft. One could venture to say that the impact of multipath would be dramatically reduced if

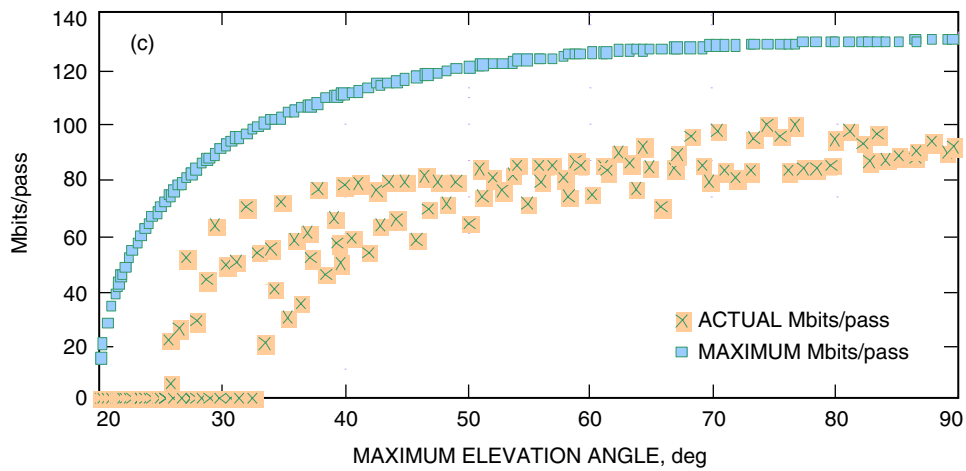
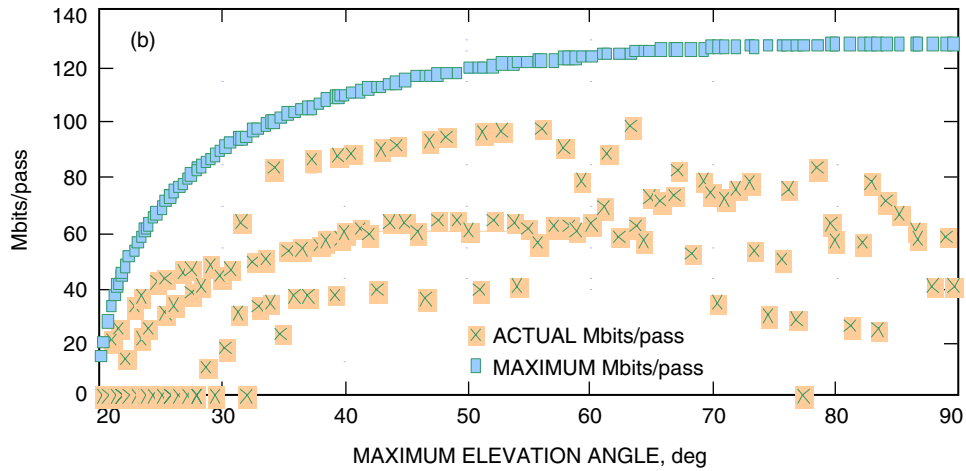
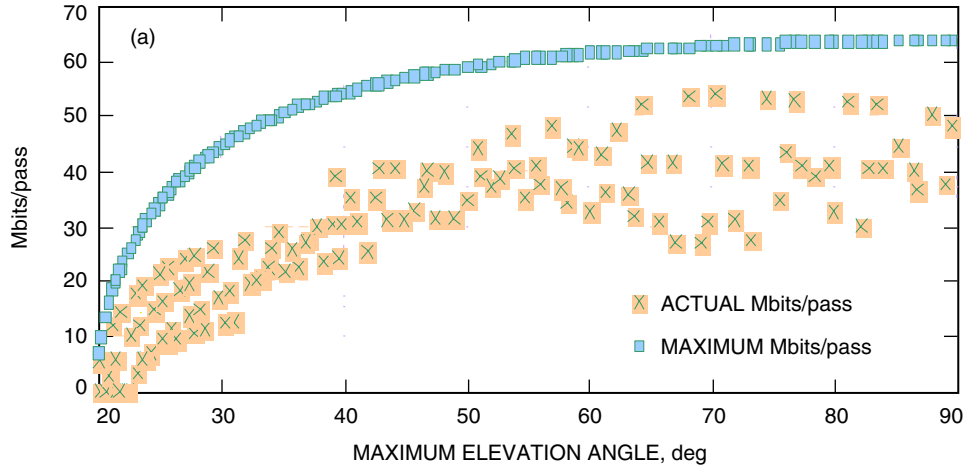


Fig. 8. Odyssey-Smart Lander, data volume per pass versus maximum elevation angle: (a) Smart Lander with solar-array-mounted monopole antenna, data rate 128 kb/s, (b) Smart Lander with equipment-deck-mounted monopole antenna, data rate 256 kb/s, and (c) Smart Lander with solar-array-mounted cross-dipole antenna, data rate 128 kb/s.

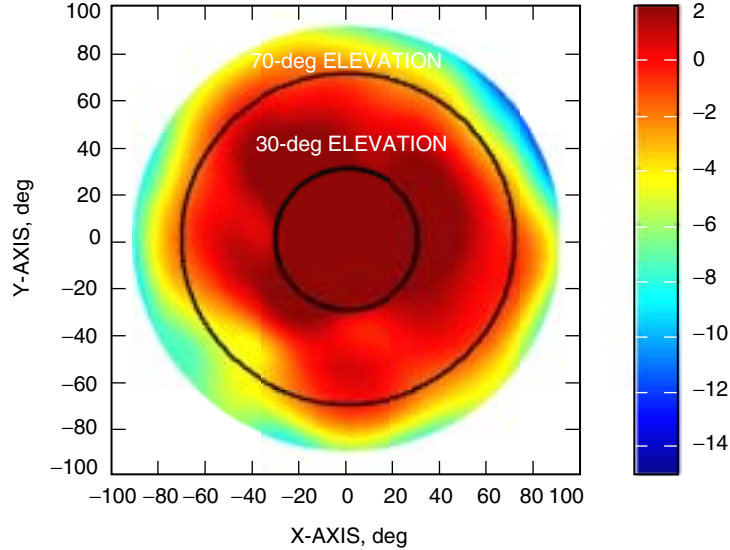


Fig. 9. Contour plot of the Odyssey quadrafilar helix antenna.

the UHF low-gain antenna were placed out on the end of a boom. It is impossible to make a specific prediction about the effect of multipath mitigation without either a computer model or test results of the antenna pattern on the end of a boom. For the purpose of our study, we assumed there were ideally symmetrical antenna patterns mounted on Centre National d'Etudes Spatiales 2007 (CNES 2007) and Odyssey and estimated the improvement in the amount of data-volume return.

Figures 10 and 11 show the antenna pattern for CNES and Odyssey, respectively. The CNES received antenna gain pattern was unknown to us at the time of performing this analysis. The CNES received antenna gain pattern was unknown to us at the time of performing this analysis, and we assumed the gain pattern of Fig. 10 based on personal communications with the telecommunications team for CNES. Figure 11 shows the gain pattern versus the off-bore-sight angle of the quadrafilar helix antenna mounted on Odyssey at 0-deg azimuth. It was assumed that the gain pattern for all azimuth angles would be identical if the multipath-induced effect were reduced to zero. Similar to the procedure described in Section II, using SOAP geometry simulations and link analysis, data volumes per sol for the CNES–Smart Lander uplink and the Odyssey–Smart Lander uplink were estimated. The gain patterns shown in Figs. 10 and 11 were assumed for the orbiters. Smart Lander uses cross-dipole antennas. It was assumed that CNES uses an Electra receiver (currently under development at JPL) with 1.8-dB circuit loss. Figure 12 shows that the average data-volume return of 336 Mbits per sol at a very high data rate of 1024 kb/s can be achieved with the CNES–Smart Lander uplink. Note that CNES uses a different receiver than does Odyssey. To understand the effect of having an antenna with a completely symmetric gain pattern on the spacecraft, the results obtained in Section II with Odyssey–Smart Lander must be compared to the result obtained from this section. Figure 13 shows that data-volume return increases 0.56 dB when the gain pattern shown in Fig. 11 rather than the gain pattern shown in Fig. 9 is placed on Odyssey. Figure 14 shows the plot of data volume per pass versus maximum elevation angle. Since the selected data rate for CNES–Smart Lander is high, passes with maximum elevation angles less than 30 deg were missed.

IV. Multipath from Mars' Environment

In this section, reflections from Mars' surface and diffraction from hills are studied. Satellite mobile propagation references usually rely on data obtained from testing of multipath on Earth, where shadowing effects dominate. However, there is no foliage on Mars and, hence, shadowing is not expected to be a

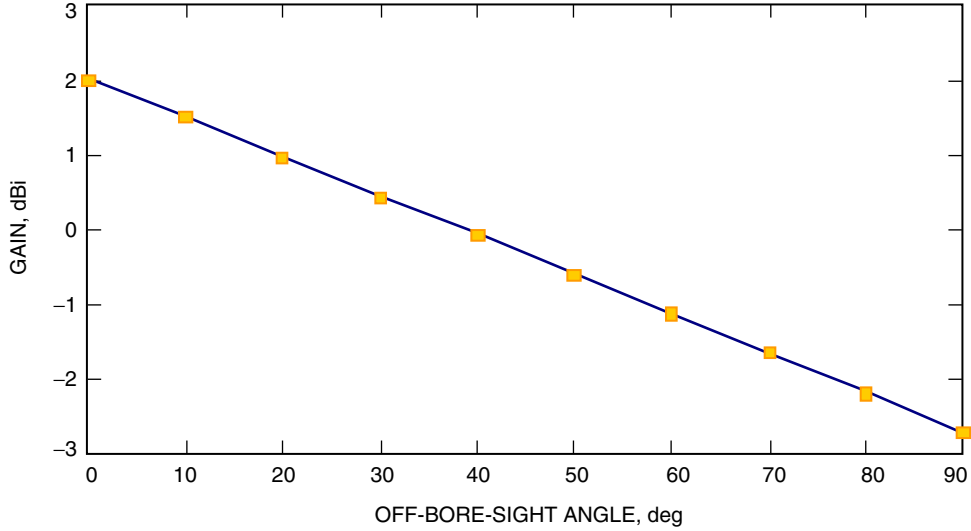


Fig. 10. CNES received antenna gain pattern with no multipath-induced effect.

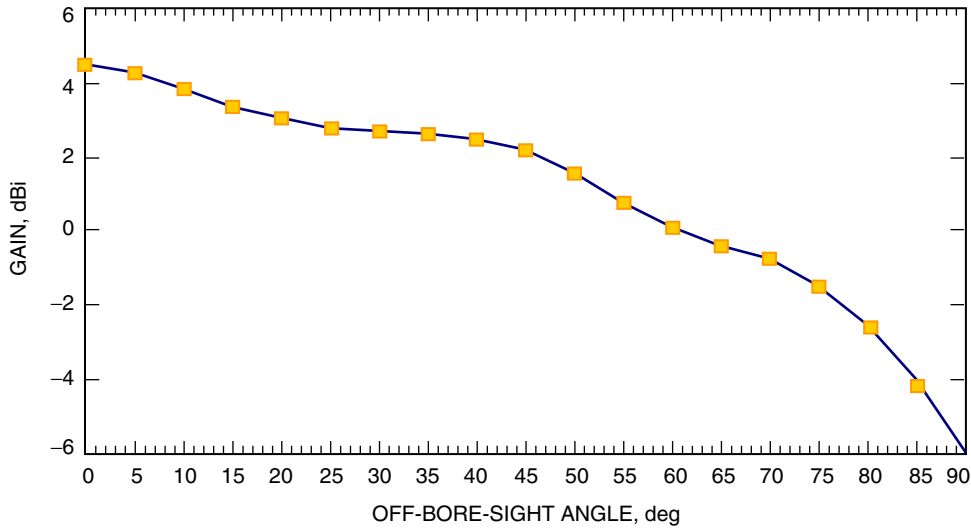


Fig. 11. Odyssey received antenna gain pattern with no multipath-induced effect.

factor. Also, most of the Earth data would be useless because of the wrong soil type. The multipath reflection coefficient depends on the soil electrical properties, incidence angle, signal frequency, and signal polarization. The permittivity coefficient of the desert is the closest to that of Mars. However, there might be little shadowing in the desert. Multipath also depends on the antenna type deployed on the top of the vehicle or rover. Therefore, it is necessary to perform a study to investigate the effect of multipath from Mars' environment on the in situ links.

A. Multipath Amplitude Reflection Coefficient for Martian Soil

Specular reflection occurs when a signal encounters a plane surface that is smooth relative to the signal wavelength. The angle of incidence will be equal to the angle of reflection. In the literature, a vertically polarized wave refers to one whose electric field vector oscillates along a line vertical to Earth. Similarly, a horizontally polarized wave is defined as one whose electric field vector oscillates along a line parallel to Earth. Horizontally polarized signals and vertically polarized signals behave differently upon

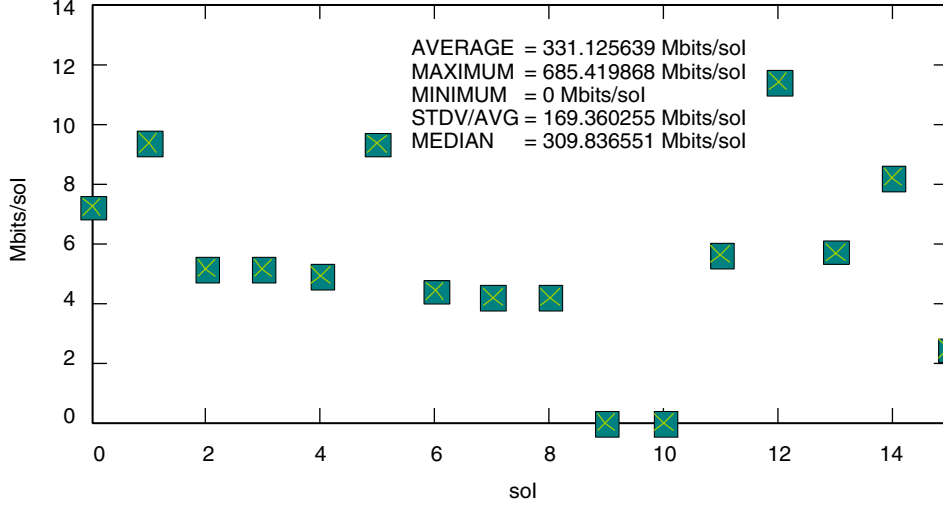


Fig 12. CNES with low-gain antenna, Smart Lander with cross-dipole antenna, data rate 1024 kb/s.

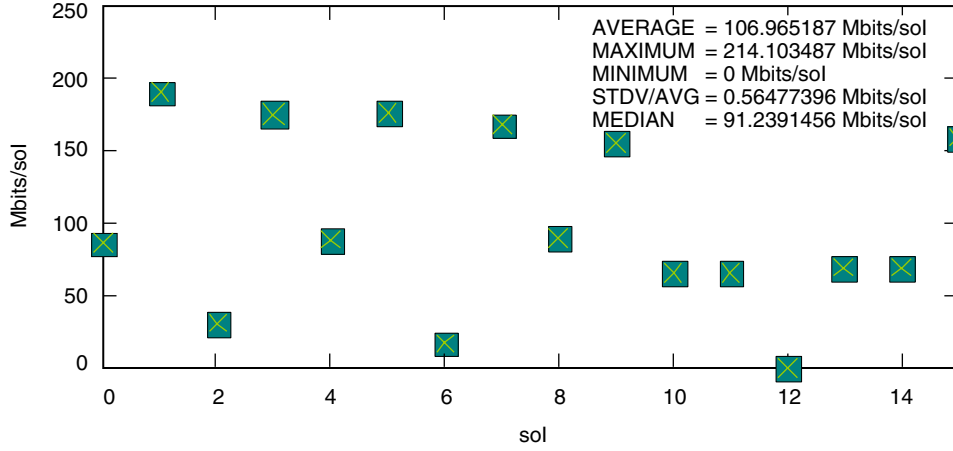


Fig 13. Odyssey with symmetric quadrafilax helix, Smart Lander with cross-dipole antenna, data rate 256 kb/s.

ground reflection. The horizontal reflection coefficient, R_H , and vertical reflection coefficient, R_V , can be obtained by [1]

$$R_H = \frac{\sin(\theta) - \sqrt{\varepsilon - \cos^2(\theta)}}{\sin(\theta) + \sqrt{\varepsilon - \cos^2(\theta)}} \quad (1)$$

$$R_V = \frac{\sin(\theta) - \frac{\sqrt{\varepsilon - \cos^2(\theta)}}{\varepsilon}}{\sin(\theta) + \frac{\sqrt{\varepsilon - \cos^2(\theta)}}{\varepsilon}} \quad (2)$$

where ε is the permittivity of the Martian soil, which was assumed to be a complex number. In [2], the permittivity and permeability of Martian soil have been given as functions of frequency. For a UHF relay link and at the transmitting frequency of 401.5 MHz, ε is approximately equal to $3.2 + j0.18$; θ is the incidence angle in radians. Figure 15 shows plots of the results.

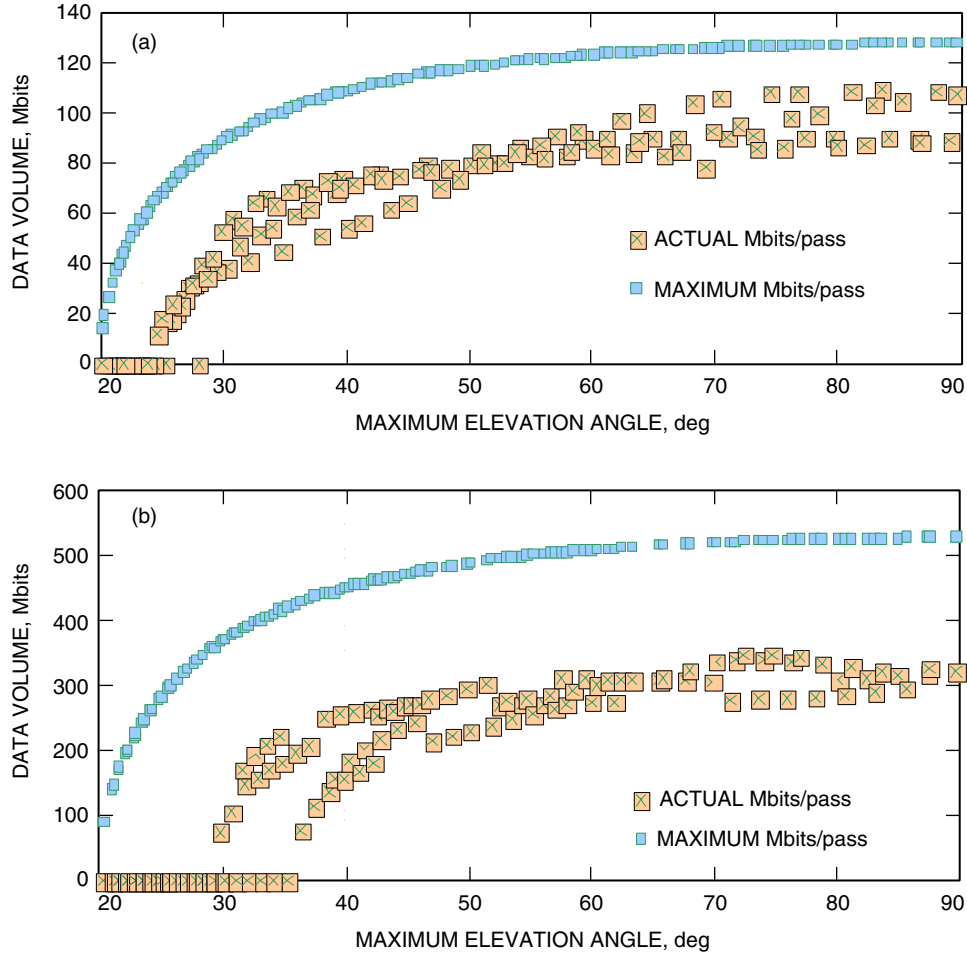


Fig. 14. Data volume per pass versus maximum elevation angle: (a) Odyssey with symmetric helix, Smart Lander with cross-dipole antenna, data rate 256 kb/s and (b) CNES with low-gain antenna, Smart Lander with cross-dipole antenna, data rate 1024 kb/s.

It is seen that the magnitude of the horizontal reflection coefficient, R_H , decreases monotonically as elevation angle increases. The phase lag of the reflected signal is nearly 180 deg for all elevation angles. The vertical reflection coefficient, R_V , behaves much differently. Between the 0-deg elevation angle and the Brewster angle, R_V decreases monotonically from 1 to 0. Above the Brewster angle, R_V increases monotonically until it is equal to the descending R_H value at a 90-deg elevation angle. In general, the magnitude of the vertical component reaches a non-zero minimum at the Brewster angle. Below the Brewster angle, the phase lag of the vertically polarized reflection coefficient is approximately 180 deg. Above the Brewster angle, the phase lag of the vertically polarized reflection coefficient is approximately 0 deg.

Because the magnitudes of R_H and R_V are not equal, except near 0-deg and 90-deg incidence angles, a reflected circularly polarized (CP) signal comes out elliptically polarized (EP). For all incidence angles, the horizontal components switch polarization. Below the Brewster angle, the vertical component switches phase also, and the result is an EP with the same sense as the incident CP signal. At the Brewster angle, the vertical component goes to a minimum. Figure 15 shows that for Martian soil R_V is near zero at the Brewster angle (about 29 deg), resulting in a nearly horizontal linear polarized signal. Above the Brewster angle, the vertical component does not switch phase, and reflection produces an EP signal with the opposite sense of the incident CP signal.

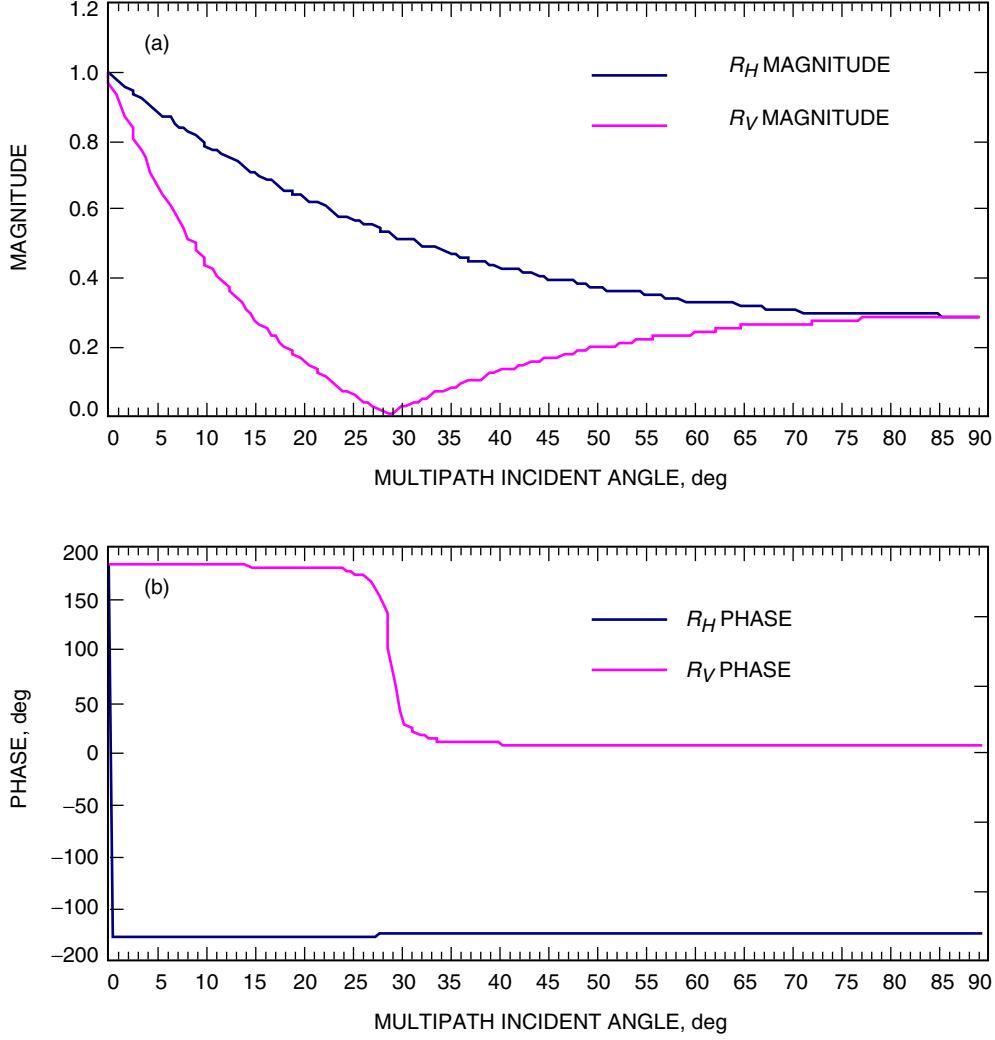


Fig. 15. Reflection coefficient of Martian soil: (a) magnitude and (b) phase.

If the incident satellite signal is circularly polarized, the specularly reflected multipath signal (from Martian soil with complex reflection coefficients) will include a co-polarized component and a cross-polarized component, where the reference polarization is that of the incident or direct signal. It is simple to calculate the circular polarization reflection coefficient from the linear reflection coefficients:

$$R_{\text{co-pol}} = R_C = \frac{(R_H + R_V)}{2} \quad (3)$$

$$R_{\text{cross-pol}} = R_X = \frac{(R_H - R_V)}{2} \quad (4)$$

The magnitudes of these two reflection coefficients are plotted in Fig. 16. If we define E_{1R} and E_{1L} , respectively, as the right-hand and left-hand component amplitudes of the incident signal, and E_{2R} and E_{2L} , respectively, as the right-hand and left-hand component amplitudes of the reflected signal, then the following relationships hold:

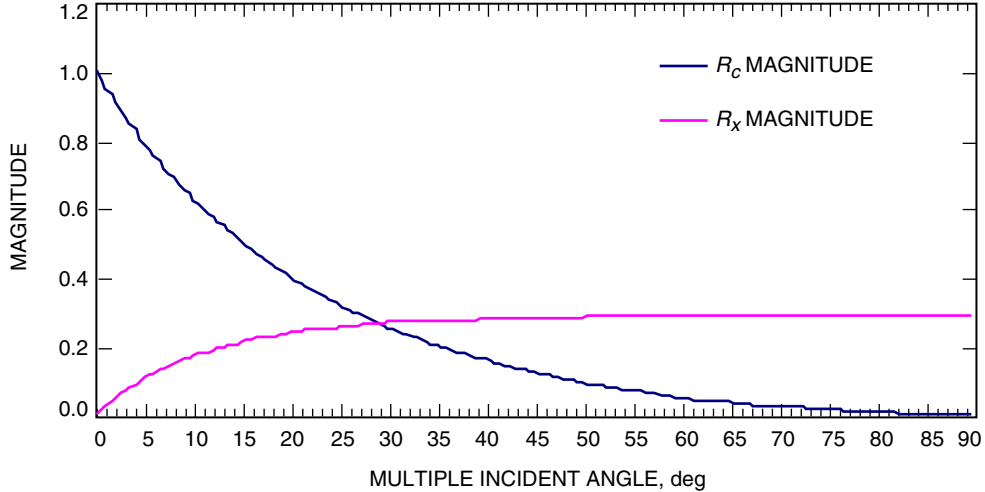


Fig. 16. Circularly polarized Martian reflection coefficient.

$$\begin{bmatrix} E_{2R} \\ E_{2L} \end{bmatrix} = \begin{bmatrix} R_C R_C \\ R_X R_X \end{bmatrix} \begin{bmatrix} E_{1R} \\ E_{1L} \end{bmatrix} \quad (5)$$

The Brewster angle now appears as the point at which the magnitude of R_C equals the magnitude of R_X . Given a pure CP signal incident at the Brewster angle, we will also find that the magnitude of the reflected co-polarization term, E_{2R} , is equal to the magnitude of the reflected cross-polarization term, E_{2L} , resulting in a net linear polarization. In summary, a pure CP incident signal produces both co- and cross-polarized reflections. Below the Brewster angle, the co-polarization component dominates. At the Brewster angle, the co-polarization magnitude exactly equals the cross-polarization magnitude. Above the Brewster angle, the cross-polarization term dominates. This interpretation will be important when we combine these reflection coefficients with the co-polarization and cross-polarization antenna patterns to determine the expected reflection component as a function of elevation angle.

There are several models suggested in the literature for multipath propagations that consider reflection, diffraction, and scattering. In this study, two simple scenarios were considered, as shown in Fig. 17: a flat, open terrain, which has specular reflection from the surface of Mars in the vicinity of the rover [Fig. 17(a)], and a hilly terrain scenario, with specular reflection due to forward scattering from the inclined terrain [Fig. 17(b)]. In both scenarios, the reflected and direct waves will combine at a given height. The magnitude of the combined signal depends on the phase difference between the reflected and direct waves. It is at maximum when the phase difference is zero and reaches its minimum when the phase difference is 180 deg.

For this simplistic case, three things determine the effect of multipath on the received signal level:

- (1) The multipath signal phase, ϕ , at the antenna relative to the direct signal component.
- (2) The horizontal and vertical polarization ground reflection coefficients. The magnitudes and signs of these reflection coefficients scale the magnitude and sign of the multipath signal. The vertical polarization coefficients will actually switch signs around the Brewster angle. For the signal-to-ground incidence angles above the Brewster angle, circular polarization will switch direction. At the Brewster angle, the vertically polarized component goes to minimum.

- (3) The antenna gain discrimination of the multipath component. Usually, the rover antenna discriminates against a Martian surface reflected signal because its gain pattern decreases below the horizon.

In actual fact, the propagation situation usually will be more complicated. The Martian surface may not be completely flat, and there may be other objects in the environment producing additional multipath components.

B. Scenario A: Multipath on Flat Terrain

Because the satellite is so far away, the elevation angle to the spacecraft remains relatively constant for all rover horizontal motions over flat, open terrain. As the rover moves, the signal path geometry remains constant, and the spacecraft position relative to the rover “appears” to move with the spacecraft. The multipath reflection points actually do move, staying a fixed distance from the rover. Since the reflection point is very near the user (because the rover height is 1 m at maximum), the multipath is termed “near-specular” reflection. For all rover horizontal motions, if the height of the antenna remains constant, the multipath signal geometry will remain constant and, thus, the fade level, assuming constant signal reflection properties, will remain constant. This assumption is valid for Martian relay links because the rover does not move when it wants to transmit or receive signals to or from the spacecraft. In actual practice, the reflection coefficients will vary somewhat and the ground will not be perfectly flat; thus, there will be some small signal variations on the order of 0 to 2 dB.

Figure 17(a) illustrates this model, where θ is the angle of the incident signal, which in turn is equal to the angle of the reflected signal. It also is equal to the elevation angle of the spacecraft over the horizon since the coming rays from the spacecraft are parallel due to the large distance between the spacecraft and the rover. The height of the receiving antenna is h . The phase delay between the direct and the reflected signals can be shown to be equal to [3]

$$\phi_1 = 2\pi f \left[\frac{h}{c \sin(\theta)} 1 - \cos(2\theta) \right] \quad (6)$$

or, equivalently,

$$\phi_1 = 2\pi f \frac{2h}{c} \sin(\theta) \quad (7)$$

where θ is the satellite elevation angle in radians, h is the height of the antenna, c is the speed of light in meters/second, and f is the frequency in hertz.

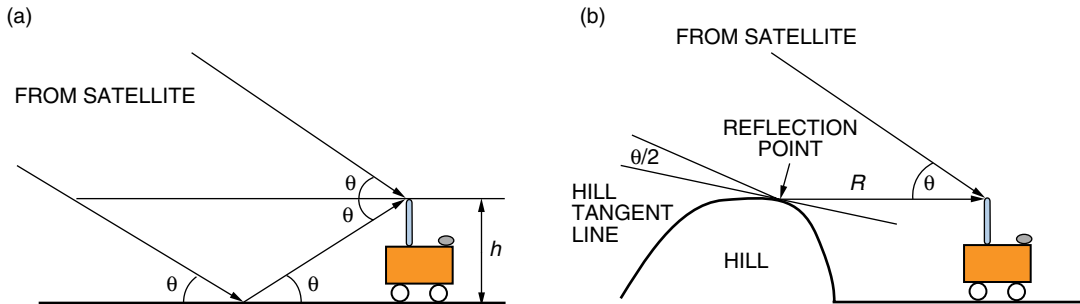


Fig. 17. Multipath geometry: (a) flat, open terrain and (b) hilly terrain.

Thus, the time delay in seconds is equal to

$$\tau_1 = \frac{\phi_1}{2\pi f} = \frac{2h}{c} \sin(\theta) \quad (8)$$

From Fig. 17(a), we can write equations to compute E_{direct} , the direct electric field, and $E_{\text{multipath}}$, the reflected electric field, in volts/meter and at elevation angle θ :

$$E_{\text{direct}} = \sqrt{G_{tc}(\theta)} \times \sqrt{G_{rc}(\theta)} \quad (9)$$

$$E_{\text{multipath}}(\theta) = \left\{ \sqrt{G_{tc}(-\theta)} \times R_c(\theta) \times \sqrt{G_{rc}(\theta)} + \sqrt{G_{tx}(-\theta)} \times R_x(\theta) \times \sqrt{G_{rx}(\theta)} \right\} \times e^{j\phi_1} \quad (10)$$

where G_{tc} and G_{tx} are transmitting co-polarized and cross-polarized component antenna gain, respectively, in watts, G_{rc} and G_{rx} are receiving co-polarized and cross-polarized component antenna gain, respectively, in watts, and R_C and R_X are complex Martian co-polarized and cross-polarized component reflection coefficients.

C. Scenario B: Multipath in Hilly Terrain

Figure 17(b) shows the multipath geometry of hilly terrain. In hilly terrain, multipath may originate from distant hills. As the user moves towards or away from the hill, the multipath appears to come from a fixed location, i.e., the distance to the multipath reflection point varies directly with the user's motion. This is different than the flat terrain case, where the multipath reflection point remained a fixed distance from the user for all other horizontal motions. We assume that the specular region has an elevation angle nearly one-half that of the incident ray. As the rover moves horizontally towards or away from the reflection point, it traverses a standing-wave pattern with a wave pattern having a wavelength that is a function of the signal wavelength and the elevation angle:

$$\lambda_{\text{standing wave}} = \frac{\lambda_{\text{transmission}}}{(1 - \cos(\theta))} \quad (11)$$

It can be shown that the time delay between the direct and multipath signals is given by [3]

$$\tau_2 = \frac{R}{c} (1 - \cos(\theta)) \quad (12)$$

where R is the distance between the rover and diffraction point in meters, as shown in Fig. 17(b), θ is the satellite elevation angle in radians, and c is the speed of light in meters/second.

Thus, the phase difference between the direct and diffracted signals is

$$\phi_2 = \frac{2\pi}{\lambda} R (1 - \cos(\theta)) \quad (13)$$

The value of R usually is on the order of tens of meters, and hence it will cause ϕ_2 to experience large fluctuations as opposed to the variation of ϕ_1 obtained for flat, open terrain. Figure 18 shows ϕ_1 and ϕ_2 versus elevation angle. It was assumed that $\lambda = 0.474$ m, $h = 1$ m for ϕ_1 , and $R = 1$ km for ϕ_2 .

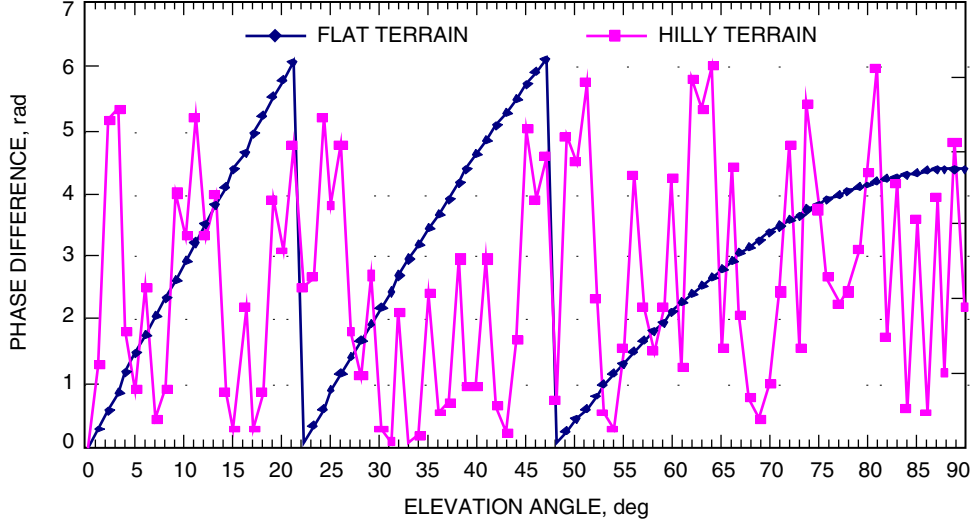


Fig. 18. Phase difference versus elevation angle.

We can derive the equations for the direct and multipath electric fields similarly to those derived for the flat, open terrain scenario. The main difference is that, for hilly terrain, the receiver sees the multipath arriving at an elevation angle near 0 deg. If the direct signal comes at an elevation angle of θ , then the multipath signal strikes the inclined hill surface at an angle of $\theta/2$, as shown in Fig. 17(b). Given this geometry, we can write

$$E_{\text{direct}} = \sqrt{G_{tc}(\theta)} \times \sqrt{G_{rc}(\theta)} \quad (14)$$

$$E_{\text{multipath}} = \left\{ \sqrt{G_{tc}(0)} \times R_c \left(\frac{\theta}{2} \right) \times \sqrt{G_{rc}(\theta)} + \sqrt{G_{tx}(0)} \times R_x \left(\frac{\theta}{2} \right) \times \sqrt{G_{rx}(\theta)} \right\} \times e^{j\phi_2} \quad (15)$$

where G_{tc} , G_{tx} , G_{rc} , G_{rx} , R_C , and R_X are the same variables as described before.

D. Case Study: Multipath for Odyssey–MER with Monopole and Cross-Dipole Antennas

The effect of reflection and scattering of Mars' environment on the uplink relay between MER and Odyssey was studied. As mentioned before, in order to include the reflected component of the electric field, the antenna gain at angles below the horizon must be available. Also, since the reflection coefficient of Mars is a complex number and R_H and R_V are not equal, it is necessary to have both co-polarized and cross-polarized antenna patterns. Therefore, a set of measurements was carried out to obtain the co-polarized and cross-polarized component patterns of the equipment-deck-mounted monopole antenna and the cross-dipole antenna on MER for a wide range of elevation angles (including the angles below the horizon) as well as azimuth angles.

On the spacecraft side, Odyssey's co-polarized component gain of 3.87 dBi and cross-polarized component gain of -10.07 dBi were plugged into Eqs. (9) and (10) and Eqs. (14) and (15). These figures correspond to the right-hand component and left-hand component gain of the Odyssey quadrafilax helix antenna at a 10-deg bore-sight offset angle.

By importing the antenna co-polarized and cross-polarized component databases into Excel and by using Eqs. (6) through (15), the direct and multipath electrical fields can be obtained as functions of elevation angle and azimuth angle. In calculating the electrical amplitudes, it was assumed that the

height of the rover and the antenna mounted on top of it is 1 m. Also, R , the distance between the diffraction point on the hill and the rover, was assumed to be 1 km.

The results are summarized in Figs. 19(a) and 19(b). As was expected, signal variation decreases as elevation angle increases. In both figures and regardless of what kind of antenna was used, the signal variation is more than 20 dB at elevation angles near 0 deg. Also, between angles of 5 to 15 deg, signal variations lie between about 2 dB and 13 dB. In flat terrain, signal variation becomes almost zero for elevation angles above 25 deg. In hilly terrain, where the multipath component is much stronger, there are still multipath components at larger elevation angles, especially with the monopole antenna mounted on the rover. This could be predicted because the cross-dipole gain pattern is more symmetric and has more discrimination at elevation angles at or below the horizon. Note that the power variation is also a function of azimuth angle. However, it was found that similar results will be obtained with different azimuth angles. The results shown in Fig. 19 are for an azimuth angle of 90 deg.

To explain the trend of power versus elevation angle, an ideal omnidirectional antenna with co-polarized and cross-polarized gains of 2 dBic and 1 dBic, respectively, was considered to be in the open, flat terrain. The result is shown in Fig. 20. Here multipath component power is much stronger, even at elevation angles

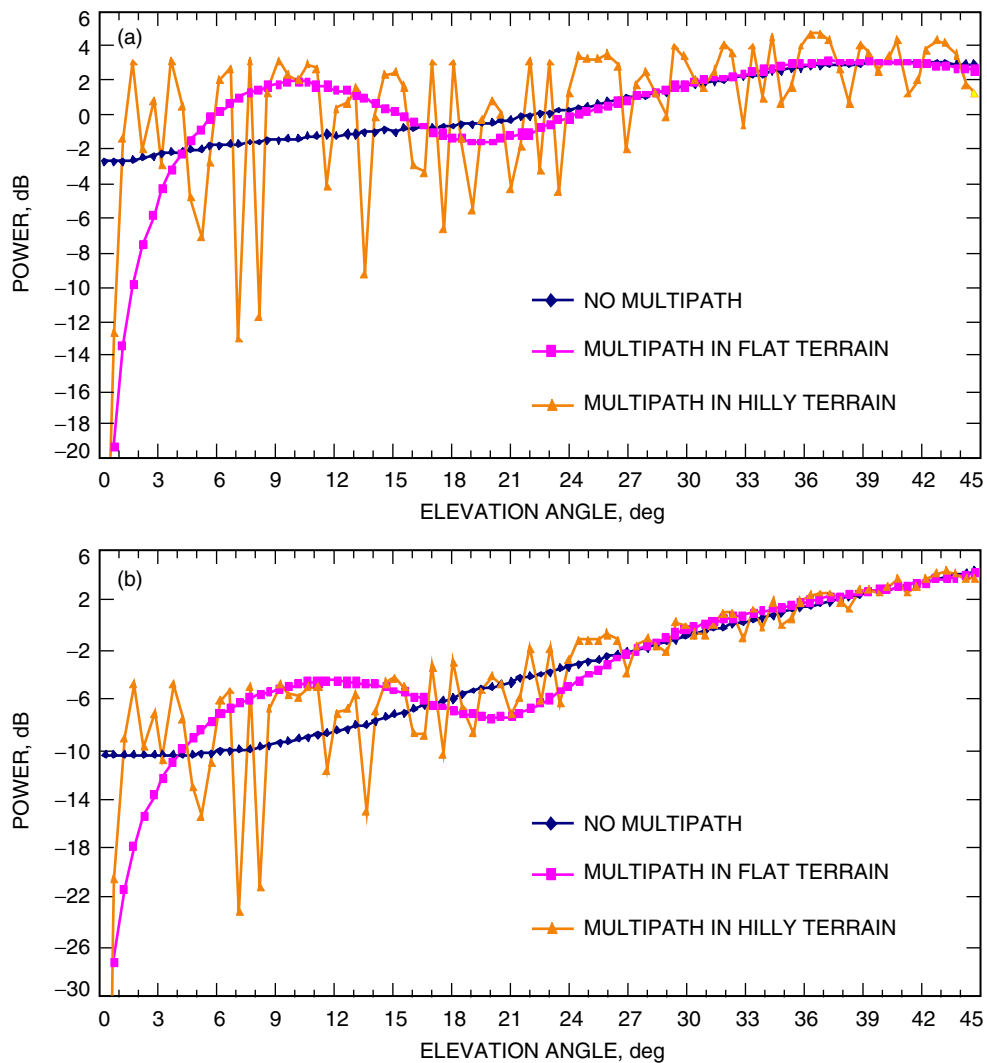


Fig. 19. Direct and total power versus elevation angle: (a) monopole antenna on MER and (b) cross-dipole antenna on MER.

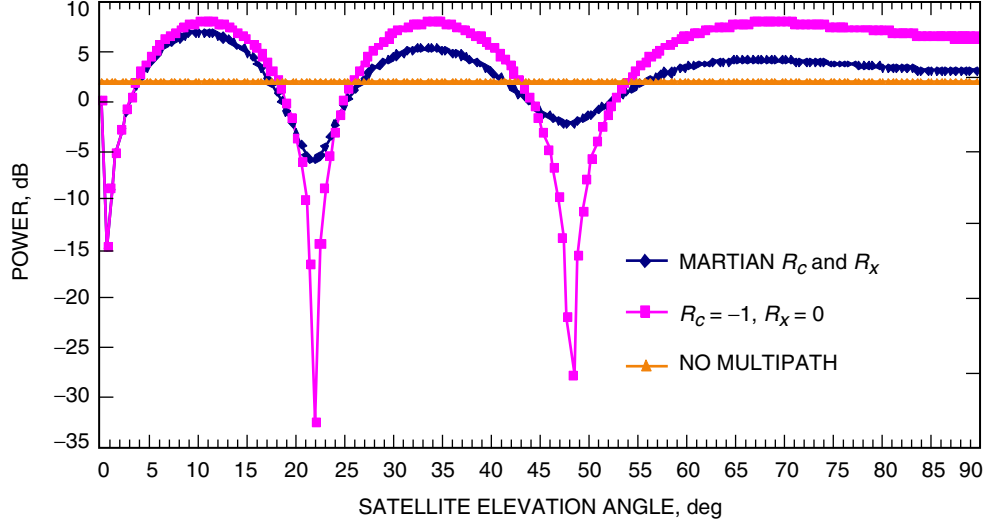


Fig. 20. Power versus elevation angle for an omnidirectional antenna.

above 30 deg, than the multipath component power shown in Fig. 19. The reason is that monopole and cross-dipole antennas discriminate against elevation angles at or below the horizon. Thus, any multipath is convolved with the specific antenna pattern mounted on the rover. In addition, the rover itself ends up blocking multipath components in many situations. Figure 20 also shows the power when the reflection coefficient is assumed to be -1 . In this case, the signal variation is even much larger compared to the Martian coefficients given in Fig. 16, in which a magnitude of R_c decreases from 1 at 0 deg to about 0 at 90 deg.

To compare the monopole and cross-dipole antennas in flat and hilly terrains, the K-factor for each case can be calculated. A combination of reflection coefficients and antenna gain pattern produces a specular k-factor, which is the ratio of direct signal to multipath signal. The specular multipath K-factor is

$$K = 20 \log_{10} \left| \frac{E_{\text{direct}}}{E_{\text{multipath}}} \right| \quad (16)$$

where E_{direct} and $E_{\text{multipath}}$ are obtained with Eq. (7) for flat, open terrain and Eq. (11) for hilly terrain. It is clear that a higher K-factor is desirable because it implies a higher ratio of $|E_{\text{direct}}/E_{\text{multipath}}|$. Figure 21 shows how the K-factor increases with an increase in satellite elevation angles for both flat and hilly terrains and at azimuth angles of 90 deg. Obviously, the amount of k-factor of hilly terrain for any given angle is less than the K-factor of flat terrain.

V. Conclusions

In this article, the effects of multipath on Martian relay link performance was studied. Section II considered multipath caused by blockage, reflection, and diffractions of mechanical equipment surrounding the antenna on the rover. Through geometry simulation in SOAP and link analysis in Excel, it was shown that data-return volume increased about 2.6 dB when a monopole antenna was placed on the equipment deck instead of on the solar arrays. Using a cross-dipole antenna with a more symmetric gain pattern instead of the equipment-deck-mounted monopole antenna increases data-volume return only 0.4 dB. Thus, most of the improvement came from placing the monopole antenna in a better location on the rover, and a smaller amount of improvement came from switching to a cross-dipole antenna. Given the

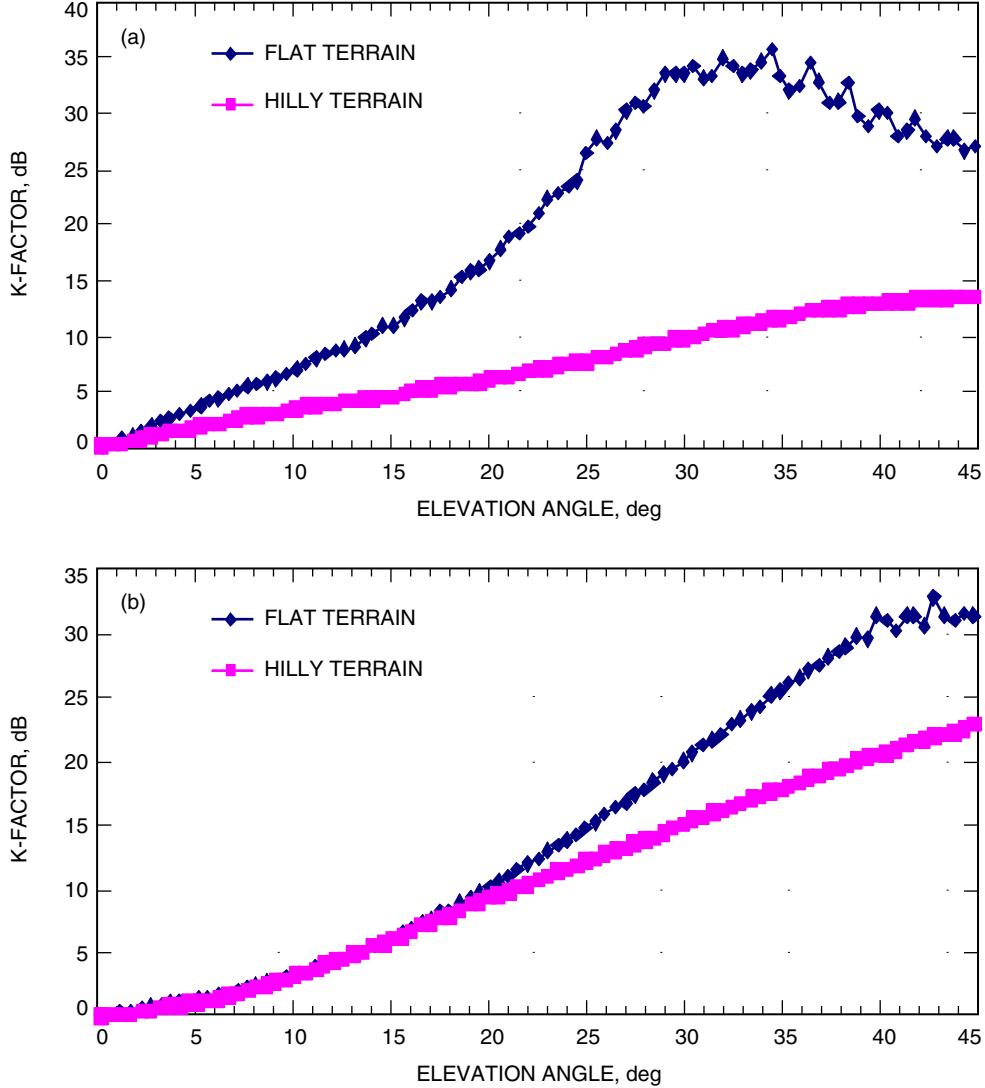


Fig. 21. K-Factor versus elevation angle: (a) monopole antenna and (b) cross-dipole antenna.

complexity of mounting a cross-dipole antenna on the rover, using a monopole antenna on the equipment deck is more economical. On the spacecraft side, the impact of a low-gain UHF antenna was studied. It was shown that a hypothetical symmetrical antenna can increase data-volume return about 0.5 dB.

In Section IV, multipath caused by reflection and diffraction from the Martian environment was considered. Our methodology was to assume simple multipath geometry models and to derive equations for direct and reflected electrical signals while taking into account the antenna gains and Martian soil reflection coefficients. Two simple environments were assumed: open, flat terrain and hilly terrain. The difference in terms of the analysis is the equation for time delay between the direct and multipath signals. Using the derived equations and the co-polarized and cross-polarized component antenna gain for the cross-dipole and monopole antennas measured on MER, variations of power versus satellite elevation angle were estimated. Despite the monopole and cross-dipole discrimination, it was shown that signal variation can reach 13 dB at elevation angles between 5 and 15 deg. Also, it was observed that using a cross-dipole antenna instead of a monopole antenna on MER decreases signal variation to 2–3 dB at elevation angles above 20 deg. Therefore, multipath on a relay link, especially at low elevation angles, is a critical parameter that should be taken into account in every future Mars mission design.

Acknowledgments

The authors would like to thank Kenneth Kelly, Joseph Vacchione, and Vaughn Cable in Section 336 for their assistance in acquiring the antenna gain pattern. We also would like to thank Christian Ho, Andrea Barbieri, and Monika Danos for their helpful discussion, and Charles Edwards for his support of this work.

References

- [1] L. Boithias, *Radio Wave Propagation*, English Translation by D. Beeson, London: North Oxford Academic Publishers, 1987.
- [2] C. Leuschen, "Analysis of the Complex Permittivity and Permeability of a Martian Soil Simulant from 10 MHz to 1 GHz," *Geoscience and Remote Sensing Symposium, 1999, IGARSS '99 Proceedings, IEEE 1999 International*, vol. 4, pp. 2264–2266, 1999.
- [3] W. J. Vogel and J. Goldhirsh, "Multipath Fading at L-band for Low Elevation Angle, Land Mobile Satellite Scenarios," *IEEE Journal on Selected Areas in Communications*, vol. 13, no. 2. pp. 197–205, February 1995.